의학박사 학위논문

Mechanism of peritumoral edema formation and relationship between weakness and demyelination in meningioma patients

—A study based on changes in diffusion parameters using diffusion tensor imaging—

수막종 환자에서 종양주위부종의 발생기전 및 수술 전 위약과 탈수초간의 연관성

—확산텐서영상을 이용한 확산계수 변화에 기초한 연구—

2012 년 8 월

서울대학교 대학원

의학과 신경외과학 과정

김명수

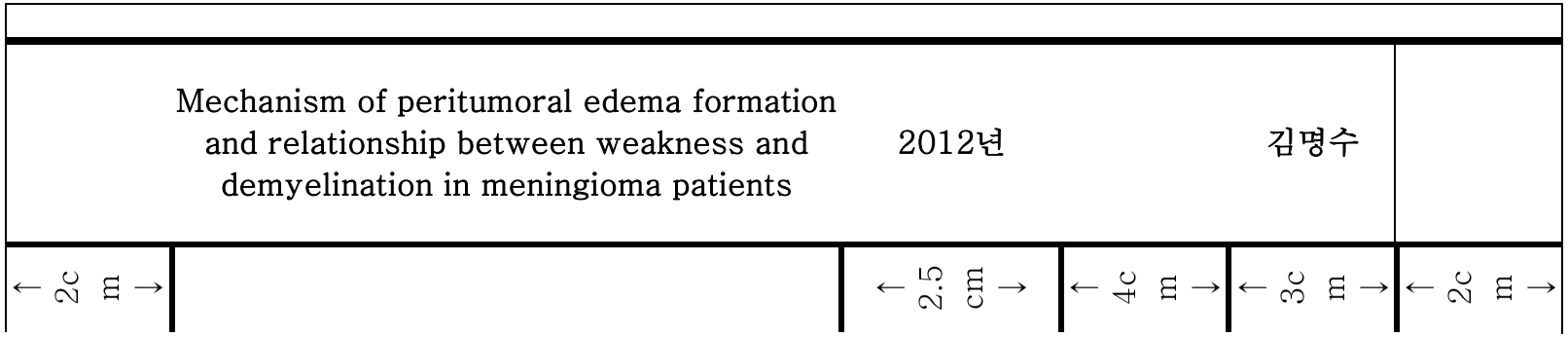
Mechanism of peritumoral edema formation and relationship between weakness and demyelination in meningioma patients
2012년
김명수
← 2cm →
← 2.5cm →
← 4cm →
← 3cm →
← 2cm →

A thesis of the Degree of Doctor of Philosophy

수막종 환자에서 종양주위부종의 발생기전 및 수술 전 위약과 탈수초간의 연관성

-확산텐서영상을 이용한 확산계수 변화에 기초한 연구-

Mechanism of peritumoral edema formation and relationship between weakness and demyelination in meningioma patients

A study based on changes in diffusion parameters using diffusion tensor imaging

August 2012

The Department of Neurosurgery

Seoul National University

College of Medicine

Myoung Soo Kim

Mechanism of peritumoral edema formation and relationship between weakness and demyelination in meningioma patients

—A study based on changes in diffusion parameters using diffusion tensor imaging—

by

Myoung Soo Kim

A thesis submitted to the Department of Neurosurgery in partial fulfillment of the requirement of the Degree of Doctor of Philosophy in Neurosurgery at Seoul National University College of Medicine

July 2012

Approved by Thesis Committee:

Professor _____Chairman

Professor _____Vice chairman

Professor _____

Professor _____

Professor _____

학위논문 원문제공 서비스에 대한 동의서

본인의 학위논문에 대하여 서울대학교가 아래와 같이 학위논문 제공하는 것에 동의합니다.

1. 동의사항

① 본인의 논문을 보존이나 인터넷 등을 통한 온라인 서비스 목적으로 복제할 경우 저작물의 내용을 변경하지 않는 범위 내에서의 복제를 허용합니다.

② 본인의 논문을 디지털화하여 인터넷 등 정보통신망을 통한 논문의 일부 또는 전부의 복제.배포 및 전송 시 무료로 제공하는 것에 동의합니다.

2. 개인(저작자)의 의무

본 논문의 저작권을 타인에게 양도하거나 또는 출판을 허락하는 등 동의 내용을 변경하고자 할 때는 소속대학(원)에 공개의 유보 또는 해지를 즉시 통보하겠습니다.

3. 서울대학교의 의무

① 서울대학교는 본 논문을 외부에 제공할 경우 저작권 보호장치(DRM)를 사용하여야 합니다.

② 서울대학교는 본 논문에 대한 공개의 유보나 해지 신청 시 즉시 처리해야 합니다.

논문 제목:

Mechanism of peritumoral edema formation and relationship between weakness and demyelination in meningioma patients

−A study based on changes in diffusion parameters using diffusion tensor imaging−

학위구분: **석사 □ · 박사 □**

학 과: Department of Neurosurgery

학 번: 2002−31135

연 락 처:

저 작 자: 김명수 (인)

제 출 일: 2012 년 08 월 일

서울대학교총장 귀하

ABSTRACT

Introduction: Diffusion tensor imaging (DTI) was recently introduced to demonstrate the diffusion properties of water molecule in brain. A reduction in diffusivity parallel to the axonal bundles (axial diffusivity [AD], $\lambda 1$) on DTI has been shown to be a specific marker of axonal damage. An increase in diffusivity perpendicular to the axonal fiber tracts (radial diffusivity [RD], $\lambda 2$ and $\lambda 3$) is a specific marker of demyelination. We analyzed the diffusion parameters of the corticospinal tract (CST), superior longitudinal fasciculus (SLF), and vasogenic edema in meningioma patients using DTI to evaluate the axonal damage and demyelination of the CST, the SLF, and vasogenic edema. And we evaluated pathogenesis of peritumoral edema formation.

Methods: Twenty-six patients with meningioma were enrolled in this study. We excluded patients with multiple meningioma and meningioma located in both hemispheres. Eleven of them with meningioma suffered from objective motor weakness and were classified as Group 1. The remaining 15 patients did not present motor weakness and were classified as Group 2. Fiber

tractography of the CST and SLF was performed, with fiber assignment by using DTIStudio (Processing Tools and Environment for Diffusion Tensor imaging, ver. 2, H Jiang and S Mori). The 26 patients with meningioma were also divided into two other groups (Group 3 and 4) according to the location of region of the interest (ROI) relative to peritumoral edema. In Group 3, the ROI was located in the peritumoral edema and in Group 4, in the normal-appearing white matter on the lesioned side. The reconstructed CST and SLF were quantitatively analyzed using the "tract statistics" function of DTIStudio. We evaluated several DTI indices (fractional anisotropy [FA], tensor trace [TT], and eigenvalues) of the CST, SLF, and vasogenic edema in patients with meningioma. The ratios (lesion side mean value/contralateral side mean value) of all diffusion values (FA, TT, and eigenvalues) of CST, SLF, and vasogenic edema on DTI were compared with 1.0 as test value using one-sample T-test.

Results: In Group 1, FA (14% decrease), TT, and RD (15%-33% increase) of the CST were significantly different between the two hemispheres but AD of the CST was not significantly different between the hemispheres. In Group 2, FA and $\lambda 3$ of

the CST did not differ significantly between the hemispheres but TT, $\lambda 1$, and $\lambda 2$ (3%−10% increase) in the CST of the ipsilateral hemisphere were significantly higher than those of the unaffected hemisphere. However, the degree of difference was small. SLF fiber tracking was performed in only 22 patients with meningioma. FA (6% decrease), TT, and RD (10%−14% increase) of the SLF differed significantly between the two hemispheres. And the differences were less than those of the CST in Group 1. AD of the SLF did not differ significantly from that in the unaffected hemisphere. In Group 3, FA (38% decrease), TT, AD, and RD (58%−171% increase) of the vasogenic edema in the hemisphere ipsilateral to the meningioma differed significantly from those in the contralateral normal−appearing hemisphere. And the differences were higher than those of the CST in Group 1 or of the SLF. In Group 4, FA, TT, AD, and RD of the ipsilateral peritumoral normal−appearing white matter did not differ significantly from those of the contralateral normal− appearing white matter.

Conclusions: Motor weakness was related to changes in FA, TT, RD, but not to changes in AD, in the CST fibers in meningioma. The diffusion parameters of the SLF in 22 meningioma patients

were similar to those of the CST in Group 1. These results are similar to those for demyelination, and suggest that the diffusion changes apparent in vasogenic edema are partly influenced by demyelination.

Keywords: Diffusion tensor imaging, Vasogenic edema, Diffusion parameter, Corticospinal tract, Superior longitudinal fasciculus

Student number: 2002-31135

The Department of Neurosurgery

Seoul National University

College of Medicine

Myoung Soo Kim

CONTENTS

LIST OF FIGURES

LIST OF ABBREVIATIONS

DTI: diffusion tensor imaging

AD: axial diffusivity

RD: radial diffusivity

CST: corticospinal tract

SLF: superior longitudinal fasciculus

ROI: region of the interest

FA: fractional anisotropy

TT: tensor trace

MR: magnetic resonance

ADC: apparent diffusion coefficient

MD: mean diffusivity

TR: repetition time

TE: echo time

V_{max}: maximum eigenvalue

PLIC: posterior limb of the internal capsule

T1: T1-weighted T2: T2-weighted

FLAIR: fluid-attenuated inversion-recovery

MC: motor cortex

SD: standard deviation

INTRODUCTION

Diffusion tensor imaging (DTI) is a magnetic resonance (MR) imaging technique that is sensitive to the diffusion properties of water molecules. The diffusion parameters describing the brain's microstructure include the three eigenvalues ($\lambda 1$, $\lambda 2$, and $\lambda 3$), directionally averaged diffusion coefficient (apparent diffusion coefficient [ADC]) and fractional anisotropy (FA). The primary eigenvalue ($\lambda 1$, axial diffusivity [AD]) is the magnitude of diffusivity in the direction of the primary eigenvector. In regions dominated by highly ordered axonal bundles, the primary eigenvalue describes the diffusivity parallel to the axonal bundles, whereas the second and third eigenvalues ($\lambda 2$ and $\lambda 3$, radial diffusivity [RD]) describe the diffusivity perpendicular to the axonal bundles. ADC is the mean of the three eigenvalues:

$$ADC = 1/3(\lambda 1 + \lambda 2 + \lambda 3)$$

The tensor trace (TT) is the sum of the three eigenvalues:

$$TT = \lambda 1 + \lambda 2 + \lambda 3$$

ADC and TT describe the spatially averaged diffusivity of water in a voxel. ADC and TT are mathematically equivalent to the

mean diffusivity (MD). FA measures the degree of directionality of diffusion within a voxel (1).

Demyelination and axonal damage are the hallmarks of white matter injury. A distinction between the two pathologic findings is important. No noninvasive biological marker that can differentiate the white matter pathological findings of demyelination from axonal damage was available until the development of DTI (2). Song et al. (3) demonstrated that the water diffusivity perpendicular to an axonal fiber (RD) was significantly higher in shiverer mice than in their age-matched controls, reflecting a lack of myelin and increased freedom of cross-fiber diffusion in the white matter. Shiverer mice are homozygous for an autosomal recessive mutation in myelin basic protein, and are characterized by incomplete myelin formation in the central nervous system. In shiverer mice, the water diffusivity parallel to the axonal fiber tracts (AD) is not altered, which is consistent with the presence of intact axons. Budde et al. (4) also suggested that a reduction in AD demonstrated with DTI is a specific marker of axonal damage in the spinal cord white matter of mice with experimental autoimmune encephalitis.

And previous DTI studies have already characterized the diffusion properties of white matter tracts in normal subjects (5). The altered states of the white matter that result from cerebral neoplasms might be expected to influence the measurement of DTI anisotropy and orientation in various ways. Intact white matter tracts displaced by a tumor might retain their anisotropy and remain identifiable in their new locations or new orientations on directional maps. Conversely, infiltrated white matter tracts might lose some anisotropy but retain their directional organization and orientation. Of course, white matter tracts might be destroyed or disrupted to the point at which their directional organization is lost completely (6).

The cerebral edema associated with tumors represents a major cause of neurological morbidity, resulting from the disruption of the normal brain anatomy and function. At present, the pathogenic mechanisms of peritumoral edema remain incompletely understood, despite many research efforts (7-10). To our knowledge, the research for directional diffusivity in white matter tract and peritumoral edema was not performed.

We analyzed the results of DTI in meningioma patients. We undertook a quantitative assessment with fiber tracking

focusing direction diffusivity. The purposes of this study were two. One was evaluation of the relationship between preoperative motor weakness and change in the diffusion parameters in the corticospinal tract (CST) of meningioma patients. Second was evaluation for mechanism of vasogenic edema formation. We examined changes in the diffusion parameter of the superior longitudinal fasciculus (SLF) and vasogenic edema to differentiate demyelination from axonal loss in the SLF and vasogenic edema of these patients.

MATERIALS AND METHODS

1. Patients

Twenty-six patients (6 men and 20 women) with meningioma were enrolled in this study. These patients had not undergone cranial surgery, brain radiation, or chemotherapy before DTI and MR imaging. We excluded patients with multiple meningiomas or meningiomas located in both hemispheres. Patients with falcine or parasagittal meningiomas located in one hemisphere were included.

Eleven patients suffered from objective motor weakness confirmed by neurological examination and were classified as Group 1. The remaining 15 patients did not report motor weakness but had other symptoms, such as headache, memory disturbance, personality change, or seizure. These patients were classified as Group 2. The tumor of all patients was confirmed pathologically. The pathological diagnoses were seven benign meningiomas, two atypical meningiomas, and two anaplastic meningiomas in Group 1, and 12 benign meningiomas and three atypical meningiomas in Group 2.

The meningiomas in Group 1 comprised three right-hemisphere lesions and eight left-hemisphere lesions. Two of

the right-sided lesions were located in the convexity and one was falcine. Of the left-sided lesions, one was located in the convexity, three were falcine, three were parasagittal, and one was located on the sphenoid ridge. The meningioma in Group 2 comprised nine right-hemisphere lesions and six left-hemisphere lesions. Of the right-sided lesions, four were located in the convexity, one was falcine, two were petroclival, and two were on the sphenoid ridge. Of the left-sided lesions, two were located on the convexity, one on the sphenoid ridge, one on the tuberculum sellae, one was parasagittal, and one was tentorial.

2. DTI data acquisition

Group I

Diffusion tensor images were acquired with a 1.5 tesla (T) MR (Signa Excite, GE, Wisconsin, USA) in two patients, 3 T MR (Signa Excite, GE, Wisconsin, USA) in four patients, and 3 T MR (Magnetom Verio, Siemens, German) in five patients, using a conventional head gradient coil. We used a single-shot spin echo-echo planar imaging sequence. The b-factor was set at 1000 s/mm^2 in seven patients and 700 s/mm^2 in four patients. The acquisition parameters used were as follows. The field of

view was 240 mm×240 mm in seven and 220 mm×220 mm in four patients. The matrix was 256×256 in all patients. The gap was 0 mm in all patients. The repetition time (TR) was 10,000-12,400 ms and the echo time (TE) was 77-86 ms. To describe the intensity and direction of the diffusion anisotropy, the MR images were acquired with 13 noncollinear diffusion gradients (total slice number 35 or 36, slice thickness 3.5 mm) and without in two patients, with 25 noncollinear diffusion gradients (total slice number 38 or 39, slice thickness 3.0 or 3.5 mm) and without in four patients, and with 30 noncollinear diffusion gradients (total slice number 60, slice thickness 1.9 mm) and without in five patients.

Group 2

Diffusion tensor images were acquired with a 1.5 T MR (Signa Excite, GE, Wisconsin, USA) in one patient, 3 T MR (Signa Excite, GE, Wisconsin, USA) in five patients, 1.5 T MR (Signa Excite HDx, GE, Wisconsin, USA) in one patient, 3 T MR (Magnetom Trio, A Tim, Siemens, German) in one patient, and 3 T MR (Magnetom Verio, Siemens, German) in seven patients, using a conventional head gradient coil. We used a single-shot spin echo-echo planar imaging sequence. The b-factor was set

at 1000 s/mm^2 in 12 patients and 700 s/mm^2 in three patients. The acquisition parameters used were as follows. The field of view was 240 mm×240 mm in 12, 230 mm×230 mm in one, and 220 mm×220 mm in two patients. The matrix was 256×256 in 14 patients and 128×128 in one patient. The gap was 0 mm in all patients. TR was 10,000–11,400 ms and TE was 74–86 ms. To describe the intensity and direction of the diffusion anisotropy, MR images were acquired with 13 noncollinear diffusion gradients (total slice number 35 or 36, slice thickness 3.5 mm) and without in two patients, with 25 noncollinear diffusion gradients (total slice number 38 or 39, slice thickness 3.0 or 3.5 mm) and without in five patients, and with 30 noncollinear diffusion gradients (total slice number 60, slice thickness 1.9 mm) and without in eight patients.

In Groups 1 and 2, from 13, 25, and 30 diffusion–weighted images, we obtained six diffusion tensor components by using multiple–order linear equations: D_{XX}, D_{YY}, D_{ZZ}, D_{XY}, D_{XZ}, and D_{YZ}. To encode the fiber tract directions, we used the maximum eigenvalue (V_{max}) of the three eigenvectors obtained by the eigen decomposition of DTI.

3. Three– dimensional CST and SLF reconstructions

Fiber tractography was performed using fiber assignment with the continuous tracking method proposed by Mori and colleagues (11). A continuous tracking algorithm using DTIStudio (Processing Tools and Environment for Diffusion Tensor Imaging, ver. 2, H Jiang and S Mori) was used in which the path follows the principal eigenvector of the diffusion tensor on a subvoxel level until the voxel edge is met, at which point the direction abruptly changes to that of the new voxel.

FA mapping was transformed into a color code: anterior to posterior, green; superior to inferior, blue; and left to right, red. The tracking algorithm was initiated from a user-defined "seed" region of interest (ROI). Tracking was initiated in both retrograde and orthograde directions according to the direction of the principal eigenvector in the ROI.

CST fiber tracking was performed in all 26 patients with meningioma. The seed ROI for the CST was the posterior limb of the internal capsule (PLIC). The target ROI was the ipsilateral cerebral peduncle. The seed and target ROIs were selected manually on directionally encoded colored or noncolored maps. Only tracts starting from the seed ROI and

passing through the target ROI were included in the trace of the CST (Figure 1).

(A)

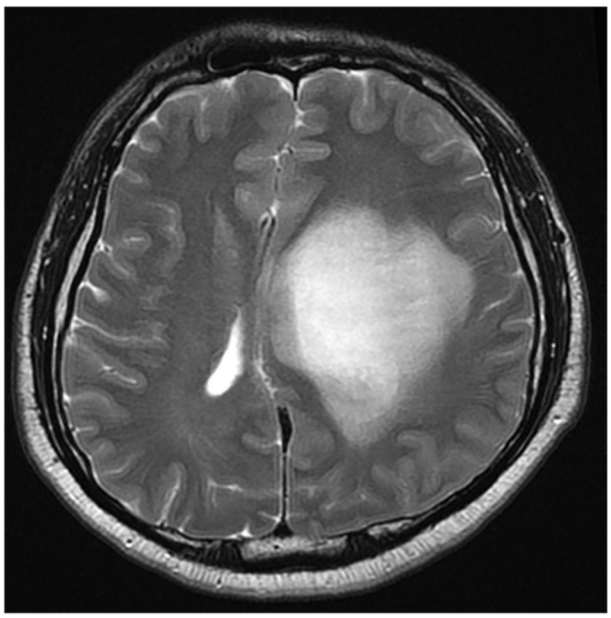

(B)

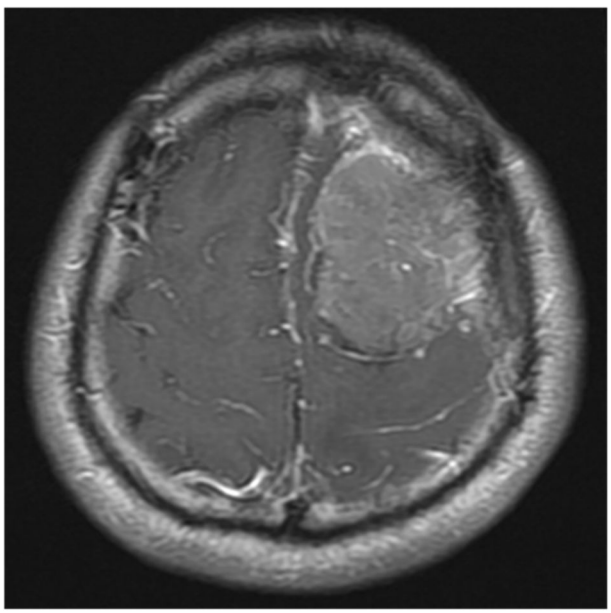

(C)

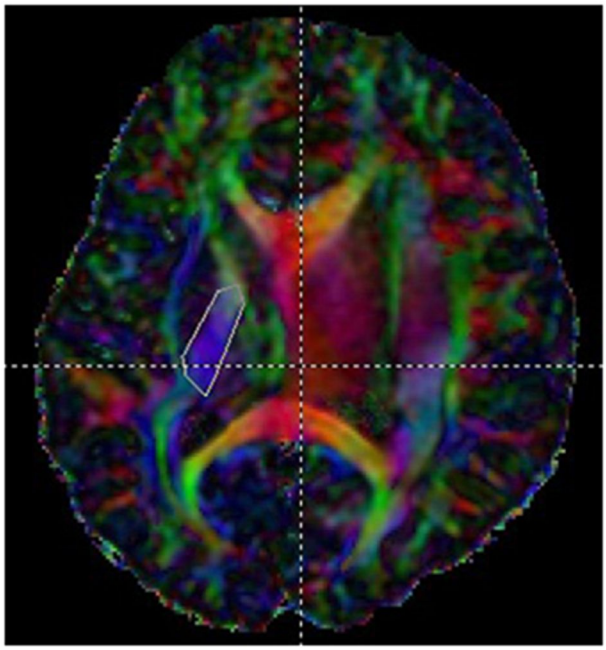

(D)

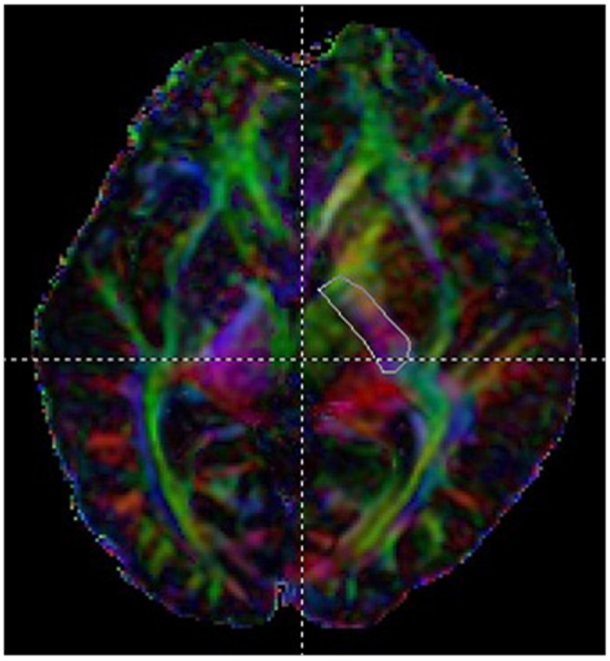

(E)

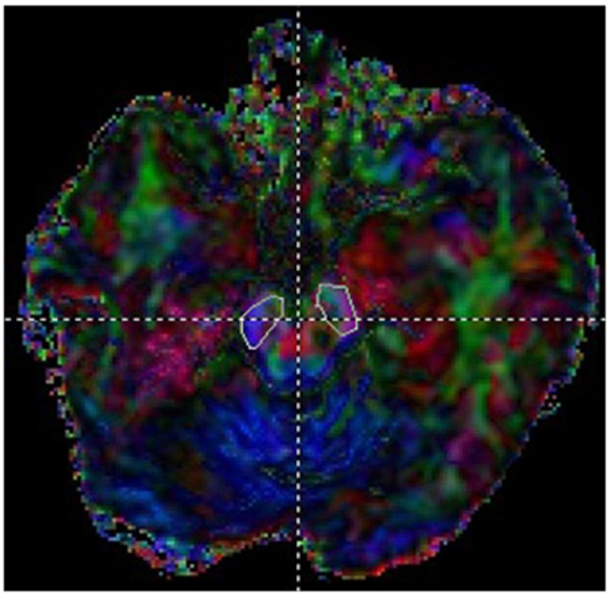

(F)

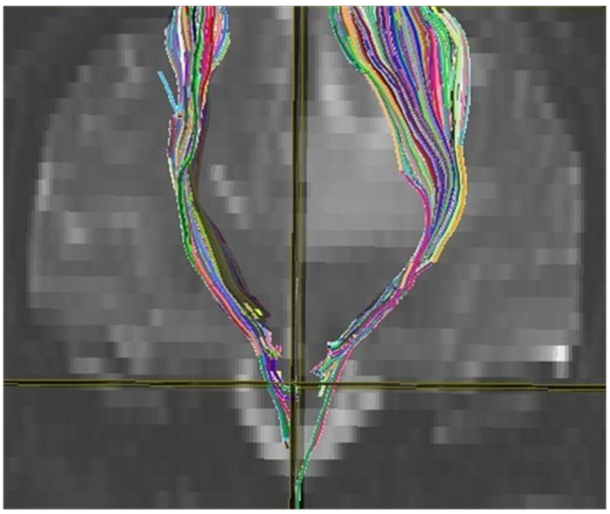

Figure 1. CST fiber tracking in a 37-year-old man with benign meningioma.

A 37-year-old man presented with seizure and right-upper-extremity weakness. T2-weighted image shows large

peritumoral edema (A). T1-enhanced image shows slightly enhanced mass in the left frontal lobe (B). The pathological diagnosis was benign meningioma. The posterior limb of the internal capsule (PLIC) is selected as the seed region of interest (ROI) (C, D). The ipsilateral cerebral peduncle is selected as the target ROI (E). The threshold level of fractional anisotropy is 0.2 in the tractography image. Tracking is terminated when the fibers show a steep turn (more than 70°). The tractography image shows the corticospinal tract on a coronal T2-weighted image (F).

SLF fiber tracking was performed in only 22 patients with meningioma. Only the seed ROI of the SLF was utilized. The seed ROI was the horizontal segment of the SLF located in the inferior parietal lobule (Figure 2). In four patients (three in Group 1 and one in Group 2), we could not identify the seed ROI because the FA value was low in this area.

(A)

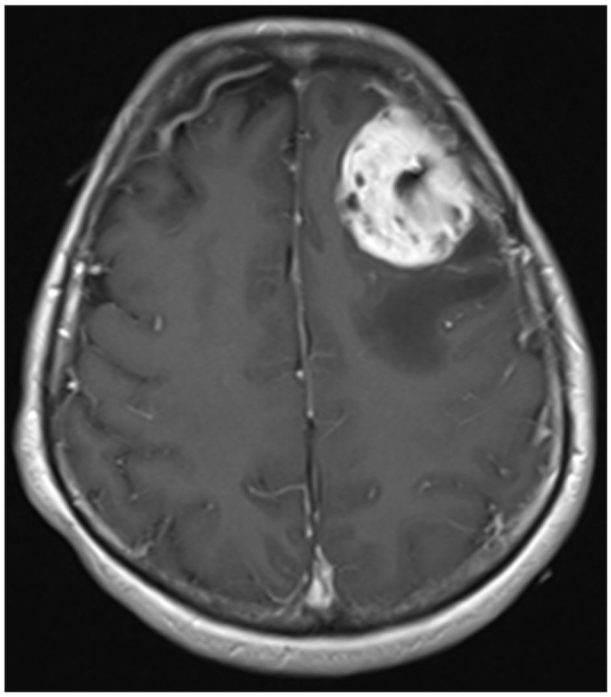

(B)

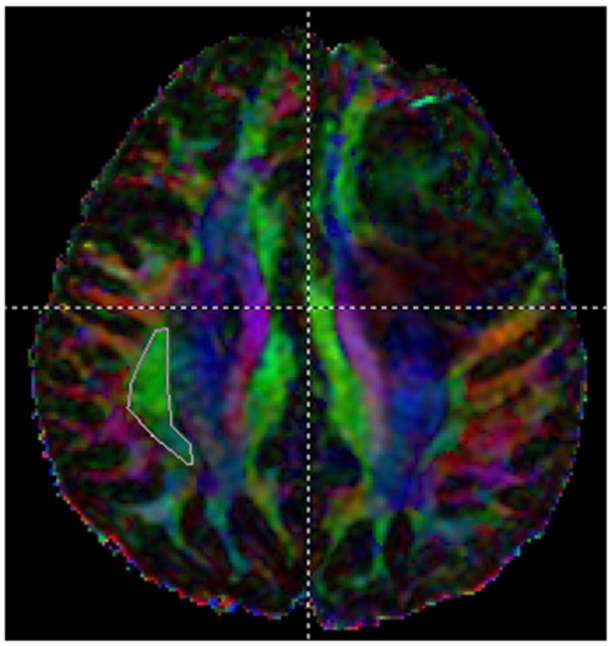

(C)

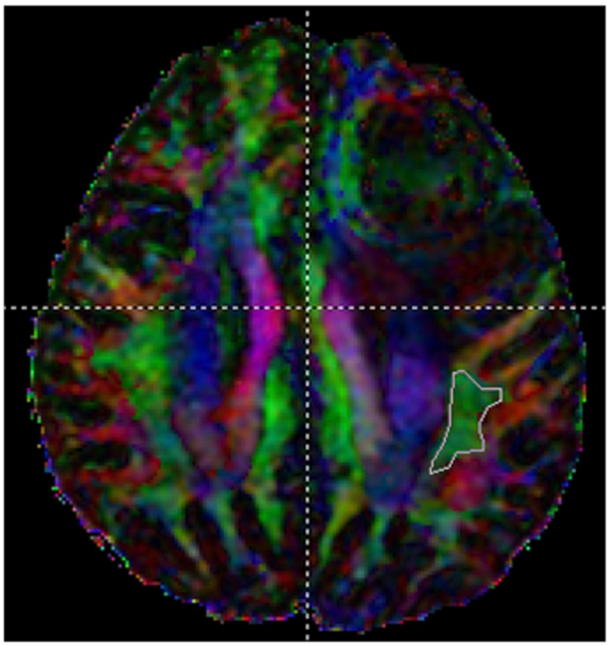

(D)

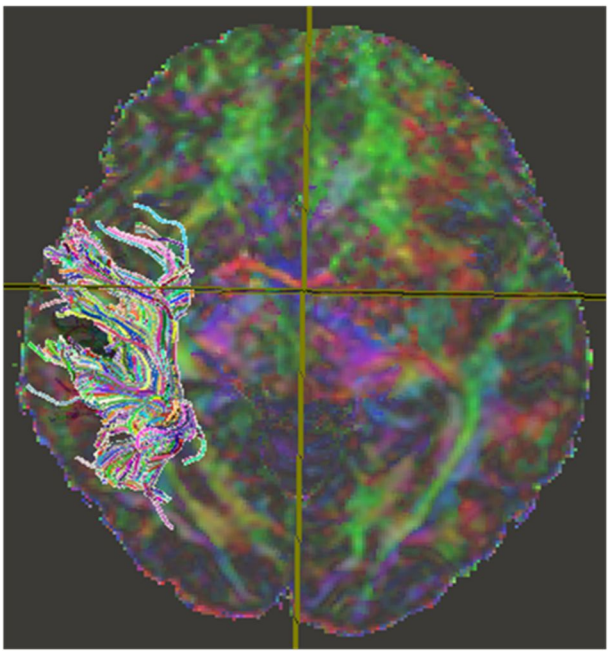

(E)

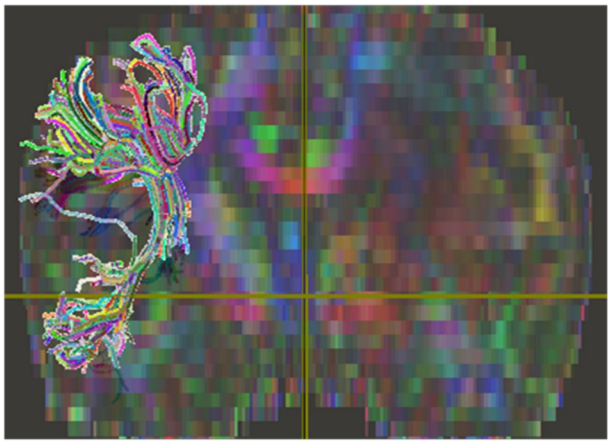

(F)

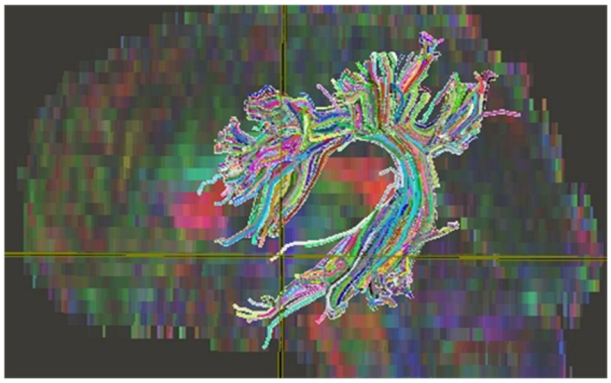

Figure 2. SLF fiber tracking in a 52-year-old woman with benign meningioma.

T1-enhanced image of a 52-year-old woman without weakness shows a left frontal convexity mass (**A**). The pathological diagnosis was benign meningioma. The seed region of interest (ROI) for tracking the right superior longitudinal fasciculus (SLF) was selected in horizontal segment of the SLF

on the right (B) and left (C) inferior parietal lobules in a color-coded fractional anisotropy (FA) map (red, left-right; blue, superior-inferior; green, anterior-posterior directions). Right SLF on tractography is illustrated in the axial (D), coronal (E), and sagittal (F) color-coded FA map.

Tracking of the CST or SLF was terminated when the fibers showed a steep turn (more than 70°). Tracking the CST or SLF was also terminated when the threshold of the FA level was below 0.2.

4. Quantitative analysis of the CST and SLF

Following anatomy-based tractography and the identification of the displaced white matter, a further quantitative analysis of the identified displaced fiber tract was performed.

FA, TT, and the three eigenvalues ($\lambda 1$, $\lambda 2$, and $\lambda 3$) of the CST and SLF were studied in all 26 and in 22 patients, respectively. Quantitative analyses of the reconstructed CST and SLF were performed using the "tract statistics" function of DTIStudio, which allows the statistical evaluation of the diffusion parameters of the reconstructed fibers.

5. Vasogenic edema evaluation

Vasogenic edema adjacent to the meningioma was divided into three grades according to the amount of edema. Grade I edema was defined as a volume less than 1/3 of the meningioma volume. Grade II was defined as a volume ranging from 1/3 to equal to that of the meningioma. Grade III was defined as a volume greater than the meningioma volume. Grade I was identified in nine patients, Grade II in six patients, and Grade III in 11 patients. We applied the ROI in the white matter of the ipsilateral and contralateral hemispheres relative to the meningioma. The size of the ROI was five times of the voxel width×five times of the voxel height (4.3 mm×4.3 mm in six patients, 4.5 mm×4.5 mm in one patient, 4.7 mm×4.7 mm in 18 patients, and 9.4 mm×9.4 mm in one patient). The 26 patients with meningioma were divided into two groups according to the ROI location relative to the edema. In 17 patients (edema Grades II and III), the ROI was located in the peritumoral edema of the hemisphere ipsilateral to the meningioma. These patients were defined as Group 3. In Group 3 patients, nine patients had motor weakness (Group 1) and eight had no motor weakness (Group 2). In nine patients (edema Grade I), the ROI was located in tumor adjacent normal-appearing white matter

of the hemisphere ipsilateral to the meningioma. These patients were classified as Group 4. In Group 4, two patients had motor weakness (Group 1) and seven had no motor weakness (Group 2). In Groups 3 and 4, the contralateral ROI was located in normal-appearing white matter in the contralateral hemisphere (Figure 3).

(A)

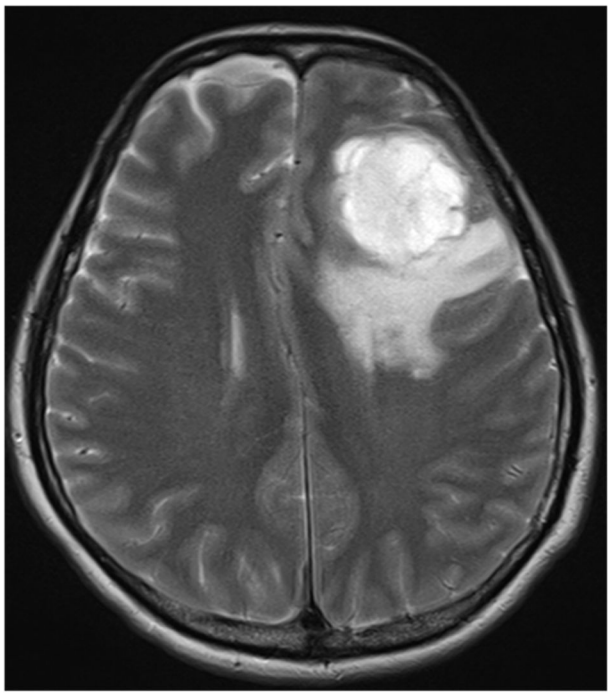

(B)

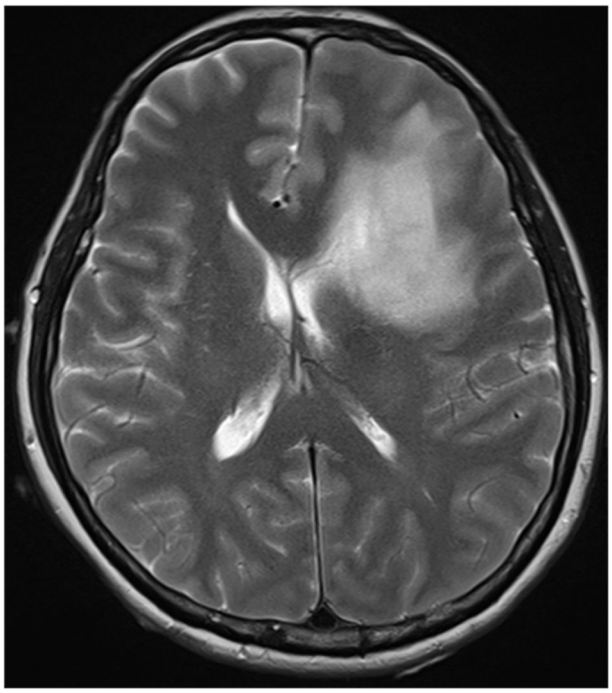

(C)

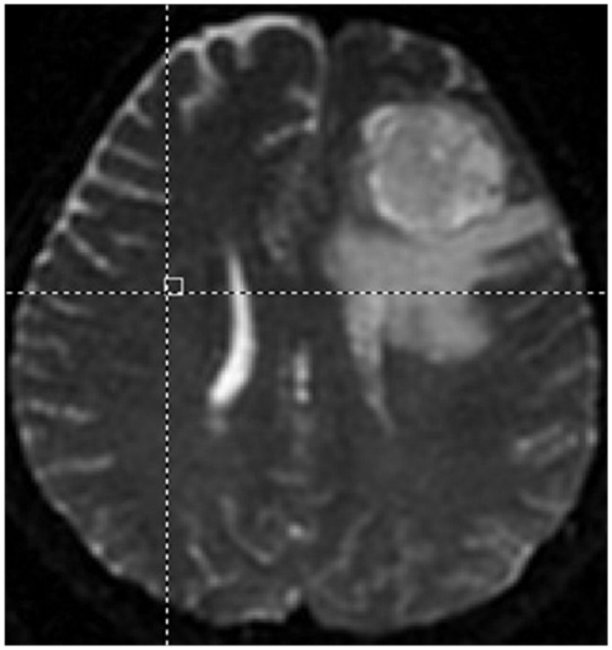

(D)

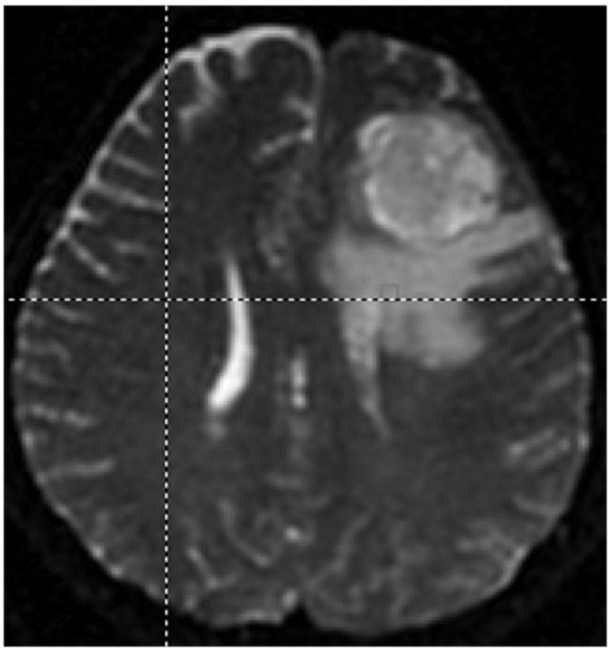

(E)

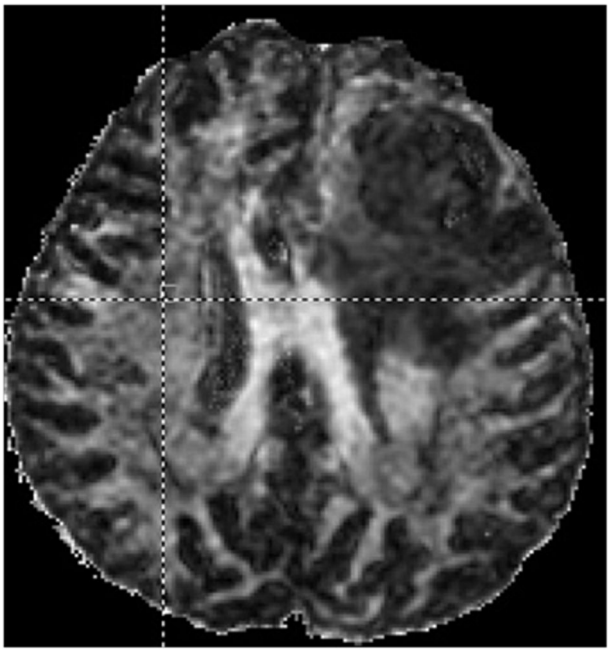

(F)

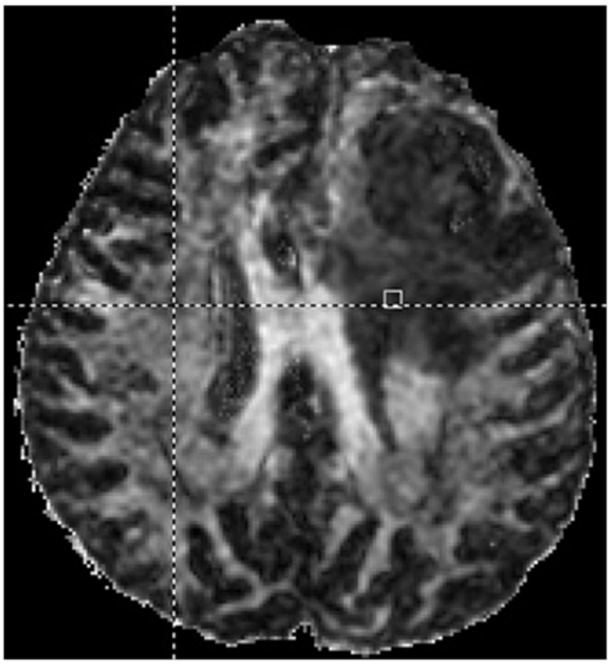

(G)

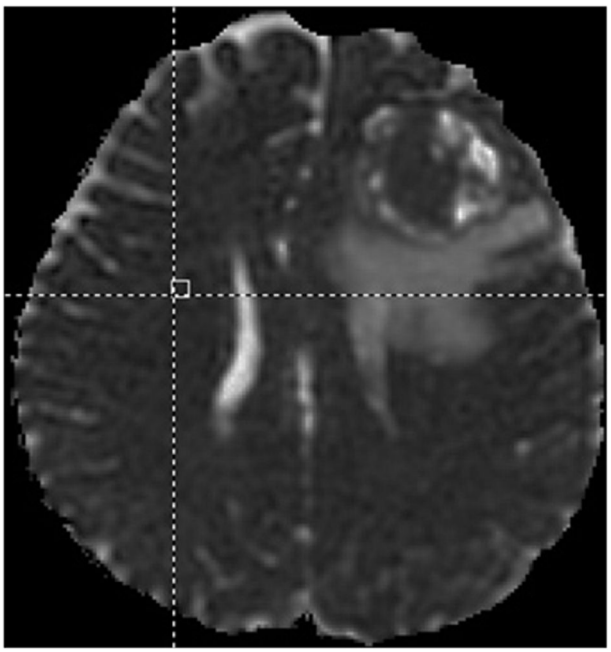

(H)

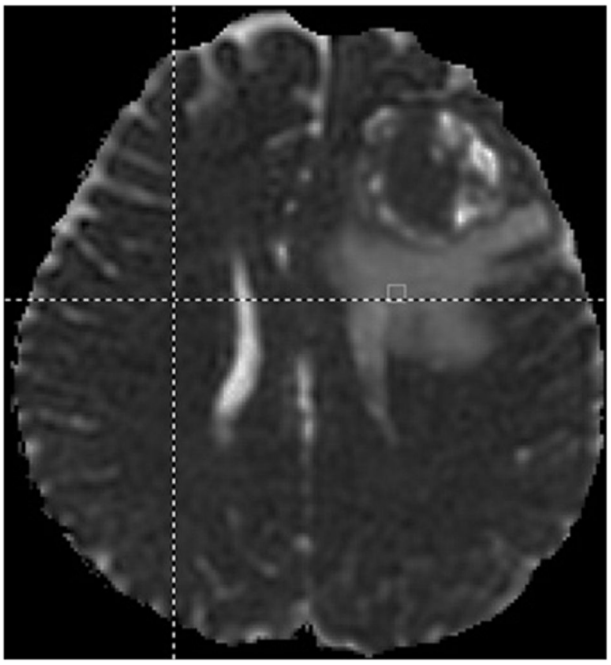

Figure 3. Diffusion parameters in vasogenic edema adjacent to the meningioma and contralateral normal-appearing white matter. T2-weighted images (**A, B**) of a 52-year-old woman without weakness show a left frontal mass associated with Grade III peritumoral edema. The pathological diagnosis was benign meningioma. Sizes of the regions of interest (ROIs) on T2-weighted image, and the fractional anisotropy (FA) and tensor trace (TT) map are 4.7 mm×4.7 mm. And positions of ROI are same in all images. Right (**C**) and left (**D**) ROIs on T2-weighted images created with diffusion tensor imaging (DTI) are located in the contralateral normal appearing white matter and in the

peritumoral edema in the hemisphere ipsilateral to the meningioma. Right (**E**) and left (**F**) ROIs in a FA map image by created with DTI are located in the contralateral normal appearing white matter and in the peritumoral edema in the hemisphere ipsilateral to meningioma, respectively. The FA ratio in the ROI (FA of lesioned side ROI/FA of contralateral side ROI) is 0.5. Right (**G**) and left (**H**) ROIs in the TT map image by created with DTI are located in the contralateral normal-appearing white matter and the ipsilateral peritumoral edema, respectively. The TT ratio in the ROI (TT of lesion ROI / TT of contralateral ROI) is 2.439.

6. FA and TT of the meningioma and contralateral white matter

To verify that the different MR units and image parameters did not significantly influence the diffusion parameters, we analyzed FA and TT of the meningiomas and the contralateral white matter.

FA and TT of the meningiomas were assessed using the method described by Toh et al. (12). The ROI was positioned manually in the solid-enhancing area of the meningioma. We

tried to exclude areas with vessel or calcification. We also evaluated the contralateral normal white matter for FA and TT. The size of the ROI in the enhancing area of the meningioma and in the contralateral normal white matter was 10 times of the voxel width×10 times of the voxel height (8.6 mm×8.6 mm in six patients, 9.0 mm×9.0 mm in one patient, 9.4 mm×9.4 mm in 18 patients, and 18.8 mm×18.8 mm in one patient). We compared the diffusion parameters (FA and TT) and the ratios of diffusion parameters between the meningioma and contralateral white matter in all 26 patients (Figure 4).

(A)

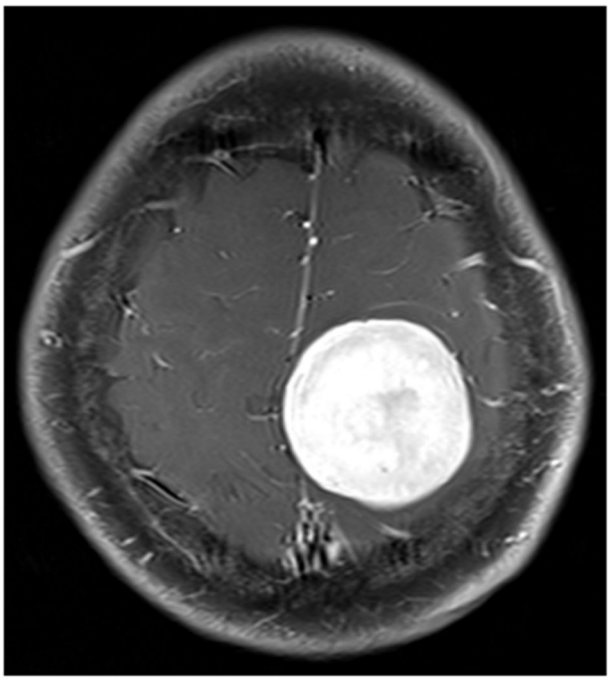

(B)

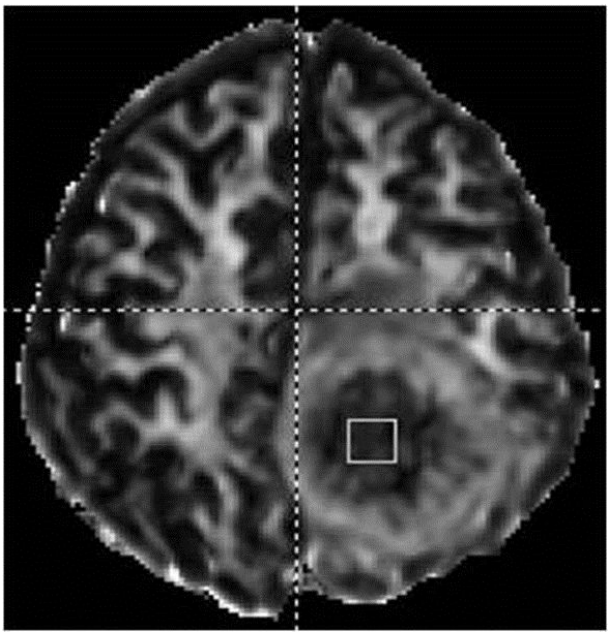

(C)

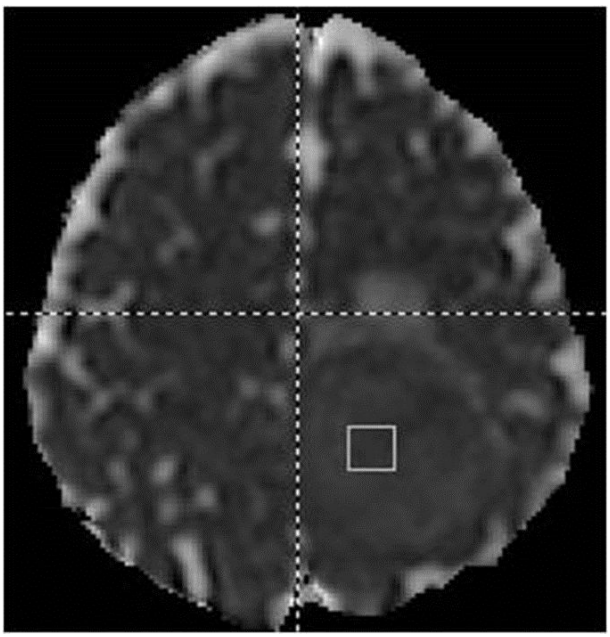

(D)

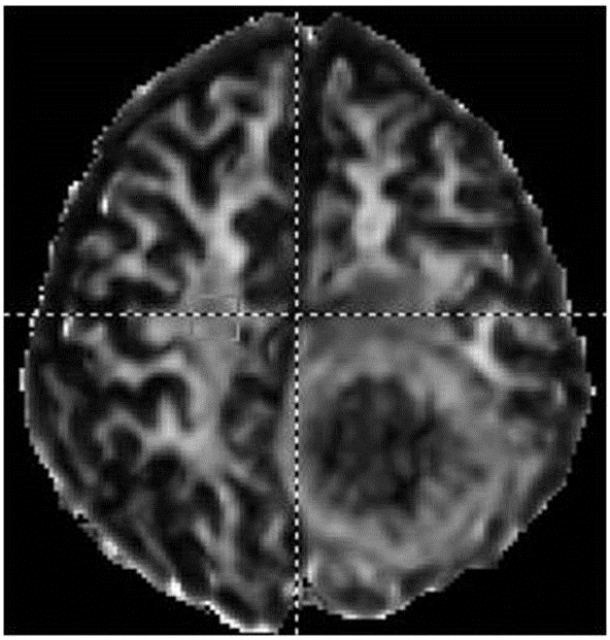

(E)

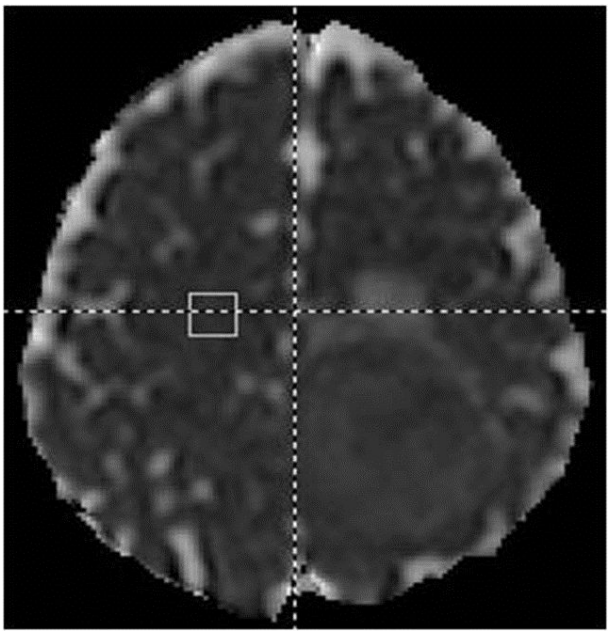

Figure 4. FA and TT in the solid-enhancing area of the meningioma and the contralateral normal white matter.

A 35-year-old woman presented with right hemiparesis. T1-enhanced image shows a strongly enhanced mass in the left hemisphere (A). The pathological diagnosis was benign meningioma. Left (B) region of interest (ROI) in the fractional anisotropy (FA) map image created with DTI is located in the solid-enhancing area of the meningioma. Left (C) ROI in the tensor trace (TT) map image created with DTI is located in the solid-enhancing area of the meningioma. Right (D) region of interest (ROI) in the FA map image created with DTI is located in the contralateral normal white matter. Right (E) ROI in the TT map image created with DTI is located in the contralateral normal white matter. The sizes of the ROIs in both the FA and TT maps are 9.4 mm×9.4 mm.

7. Conventional MR imaging evaluation

Group 1

TR and TE were as follows: 389–558 ms and 7–19 ms, respectively, for T1-weighted (T1) images; 3,986–5,160 ms and 91–129 ms, respectively, for T2-weighted (T2) images; and 8,802–11,000 ms and 95–163 ms, respectively, for fluid-attenuated inversion-recovery (FLAIR) images.

Group 2

TR and TE were as follows: 195–650 ms and 4–17 ms, respectively, for T1 images; 4,000–5,983 ms and 91–161 ms, respectively, for T2 images; and 7,502–11,600 ms and 97–174 ms, respectively, for FLAIR images.

In Groups 1 and 2, we analyzed the changes in the motor cortex (MC) on T2 images to evaluate weakness. If we found no changes in the MC, we analyzed the PLIC and cerebral peduncle.

8. Statistical analysis

Tumor size and patient's age were compared between Groups 1 and 2, and between Groups 3 and 4 using the Mann-Whitney *U*-test. The ratios (lesioned side mean value/contralateral side mean value) of all the diffusion values (FA, TT, and eigenvalues) for the CST, SLF, and vasogenic edema on DTI were compared with 1.0 as test value using a

one-sample T-test. The statistical analysis of the meningiomas was performed with the SPSS software package (version 14.0 SPSS, Inc.). Statistical significance was accepted for probability values of less than 0.05.

RESULTS

All the diffusion parameters for the meningiomas are presented as graphs (Figures 5−13). All data were presented as mean±standard deviation (SD). In each graph, the values represented by the vertical line and box are as follows: lowest level of the vertical line is the lowest value for the ratio lesion/contralateral; highest level of the vertical line is the highest value for the ratio; bottom of the box is the mean one SD of the ratio; top of the box is the mean+one SD of the ratio.

1. Demographics of the patients

In Group 1, the mean (±SD) age of the 11 patients was 54.36±16.20 years, with a range of 38−83 years. In Group 2, the mean (±SD) age of the 15 patients was 53.47±15.13 years, with a range of 26−77 years. The difference in age between two groups was not significant (p=0.856). In Group 1, the mean (±SD) tumor size for the 11 patients was 4.17±1.40 cm, with a range of 2.0−6.8 cm. In Group 2, the mean (±SD) tumor size for the 15 patients was 3.90±1.29 cm, with a range of 2.0−7.4 cm. The difference in tumor size between two groups was not significant (p=0.514).

2. FA, TT, and eigenvalues for the CST

In Group 1, FA of the CST in the hemisphere ipsilateral to the meningioma was significantly lower than that in the contralateral hemisphere (about 14% decrease). AD ($\lambda 1$) of the CST in Group 1 did not differ significantly between the hemispheres (p= 0.104). In Group 1, TT and RD ($\lambda 2$ and $\lambda 3$) for the CST in the hemisphere affected by the meningioma were significantly higher than those for the unaffected hemisphere (about 15%– 33% increase) (Figure 5).

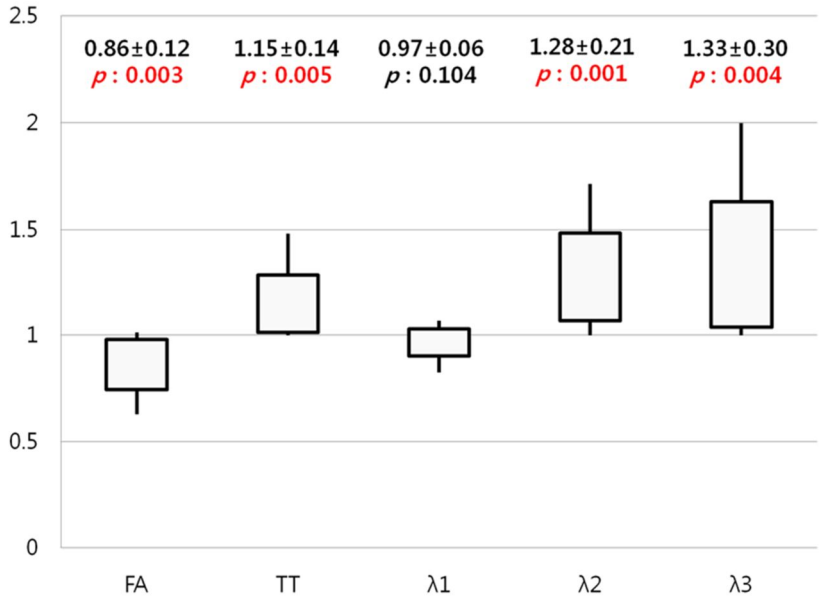

Figure 5. Ratios (lesion/contralateral) of the diffusion parameters (FA, TT, $\lambda 1$, $\lambda 2$, and $\lambda 3$) for the CST in meningioma patients with weakness (Group 1).

FA of the lesioned-hemisphere CST was significantly lower than that of the contralateral side. TT, $\lambda 2$, and $\lambda 3$ of the lesioned-hemisphere CST were significantly higher than those of the contralateral side. The axial diffusivity ($\lambda 1$) of the CST did not differ significantly between the two hemispheres.

(y axis : ratio of diffusion parameters for the CST in the two hemispheres, FA : fractional anisotropy, TT : tensor trace, $\lambda 1$: primary eigenvalue, $\lambda 2$: second eigenvalue, $\lambda 3$: third eigenvalue)

In Group 2, FA and $\lambda 3$ of CST did not differ significantly between the two hemispheres, whereas TT, $\lambda 1$, and $\lambda 2$ in the CST of the ipsilateral hemisphere were significantly higher than those of the unaffected hemisphere. But the degree of difference was small (range of 3%-10% increase) (Figure 6).

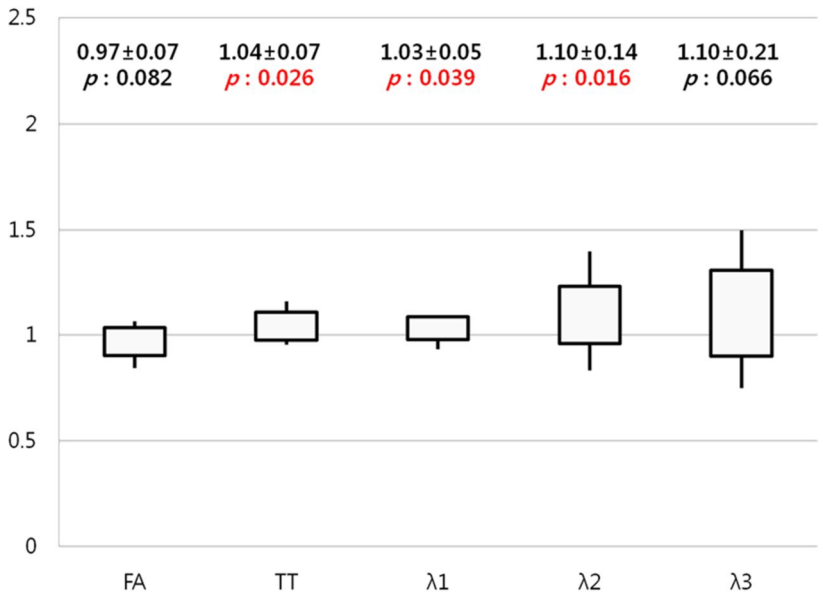

Figure 6. Ratios (lesion/contralateral) of diffusion parameters (FA, TT, $\lambda 1$, $\lambda 2$, and $\lambda 3$) for the CST in meningioma patients without weakness (Group 2).

FA and $\lambda 3$ for the CST did not differ significantly between the two hemispheres. TT, $\lambda 1$, and $\lambda 2$ of the lesion side CST were significant higher than those of the contralateral side. However, these differences were small (3%−10%).

(y axis : ratio of diffusion parameters for the CST in the two hemispheres, FA : fractional anisotropy, TT : tensor trace, $\lambda 1$: primary eigenvalue, $\lambda 2$: second eigenvalue, $\lambda 3$: third eigenvalue)

3. FA, TT, and eigenvalues for the SLF

In 22 patients with meningioma, FA of the SLF in hemisphere ipsilateral to the meningioma was significantly lower than that in the contralateral hemisphere (about 6% [1−0.94] decrease). AD of the ipsilateral SLF in 22 patients with meningioma did not differ significantly from that in the unaffected hemisphere. TT and RD of the SLF in the affected hemisphere were significantly higher than those in the unaffected hemisphere (about 10%−14% increase) (Figure 7).

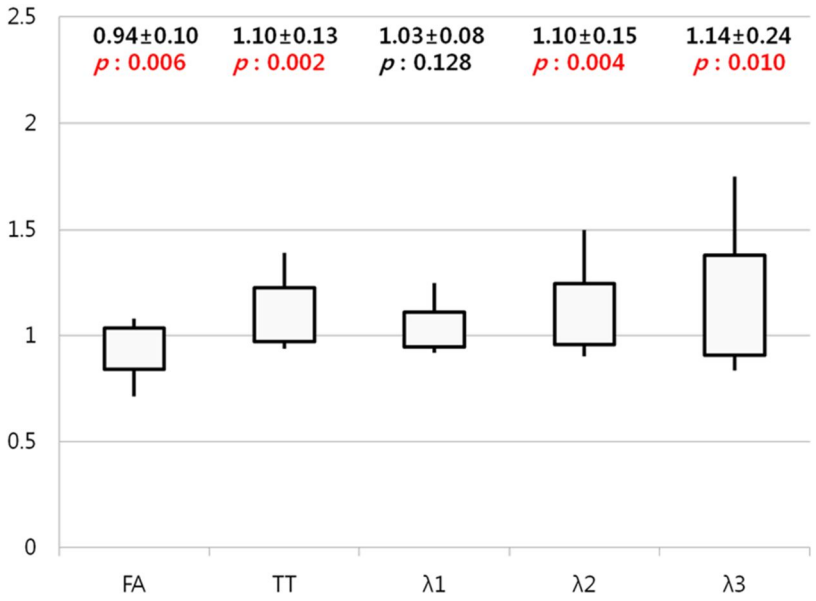

Figure 7. Ratios (lesion/contralateral) of the diffusion parameters (FA, TT, $\lambda 1$, $\lambda 2$, and $\lambda 3$) for the superior longitudinal fasciculus (SLF) in 22 patients with meningioma.

FA of the lesioned-hemisphere SLF was significantly lower than that of the contralateral side. TT, $\lambda 2$, and $\lambda 3$ of the lesioned-hemisphere SLF were significantly higher than those of the contralateral side. The axial diffusivity ($\lambda 1$) of the SLF did not differ significantly between the two hemispheres.

(y axis : ratio of the diffusion parameters for the SLF in the two hemispheres, FA : fractional anisotropy, TT : tensor trace, $\lambda 1$: primary eigenvalue, $\lambda 2$: second eigenvalue, $\lambda 3$: third eigenvalue)

4. Vasogenic edema

In Group 3, the mean (±SD) age of the 17 patients was 56.65±17.78 years, with a range of 26-83 years. In Group 4, the mean (±SD) age of the nine patients was 52.11±10.72 years, with a range of 39-71 years. The difference in age between the two groups was not significant (p=0.492). In Group 3, the mean (±SD) tumor size of the 17 patients was 4.18±1.46 cm, with a range of 2.0-7.4 cm. In Group 4, the mean (±SD) tumor size of the nine patients was 3.71±1.02 cm, with a range of 2.0-4.0 cm. The difference in the tumor sizes of the two groups was not different (p=0.404).

In Group 3, FA of the vasogenic edema in the hemisphere ipsilateral to the meningioma was significantly lower than that in the contralateral normal-appearing white matter (about 38% [1-0.62] decrease). In Group 3, TT, AD, and RD of the vasogenic edema in the affected hemisphere were significantly higher than those in the unaffected hemisphere (about 58%-171% increase) (Figure 8).

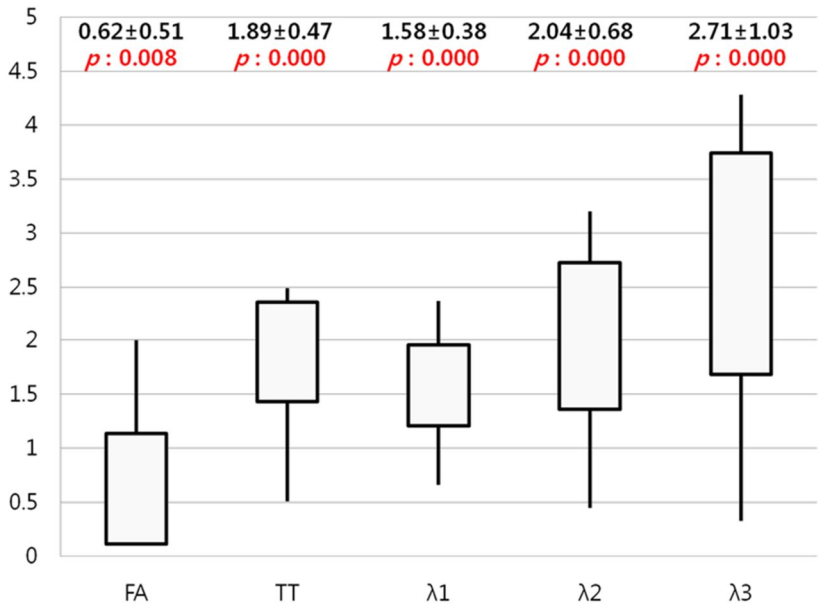

Figure 8. Ratios (lesion/contralateral) of the diffusion parameters (FA, TT, λ1, λ2, and λ3) for the peritumoral edema in meningioma patients (Group 3).

FA of lesioned-hemisphere edema was significantly lower than

that of the contralateral normal-appearing white matter. TT, λ1, λ2, and λ3 of lesioned-hemisphere edema were significantly higher than those of the contralateral normal-appearing white matter.

(y axis : ratio of diffusion parameters for the edema on the ipsilateral side and the contralateral normal-appearing white matter, FA : fractional anisotropy, TT : tensor trace, λ1 : primary eigenvalue, λ2 : second eigenvalue, λ3 : third eigenvalue)

In Group 4, FA, TT, AD and RD of the white matter without edema adjacent to the meningioma did not differ significantly from those of the contralateral hemisphere (Figure 9).

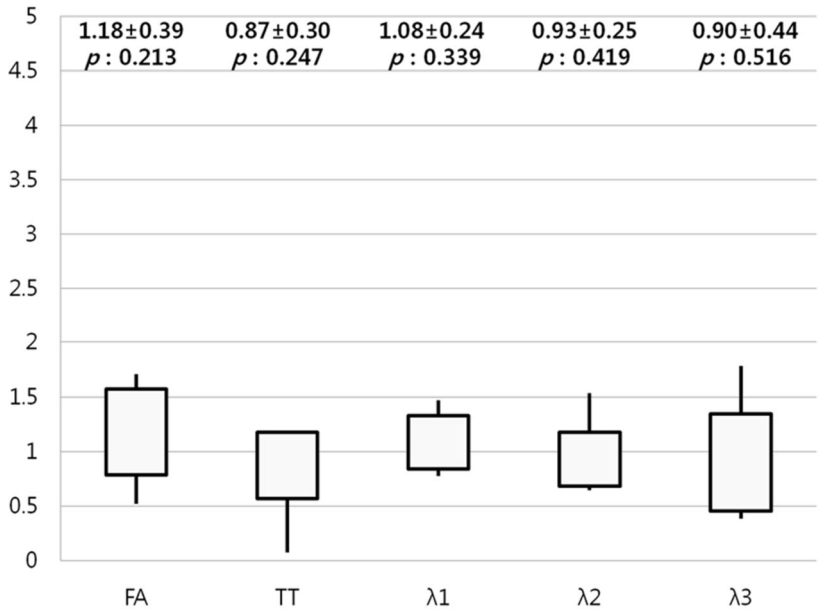

Figure 9. Ratios (lesion/contralateral) of the diffusion parameters (FA, TT, $\lambda 1$, $\lambda 2$, and $\lambda 3$) for the normal-appearing white matter in the meningioma patients (Group 4).

FA, TT, $\lambda 1$, $\lambda 2$, and $\lambda 3$ did not differ significantly across the two hemispheres.

(y axis : ratio of diffusion parameters between normal-appearing white matter in the two hemispheres, FA : fractional anisotropy, TT : tensor trace, $\lambda 1$: primary eigenvalue, $\lambda 2$: second eigenvalue, $\lambda 3$: third eigenvalue)

5. FA and TT of the meningioma and contralateral normal white matter.

FA and TT of the meningiomas are presented in Figures 10 and 11, respectively.

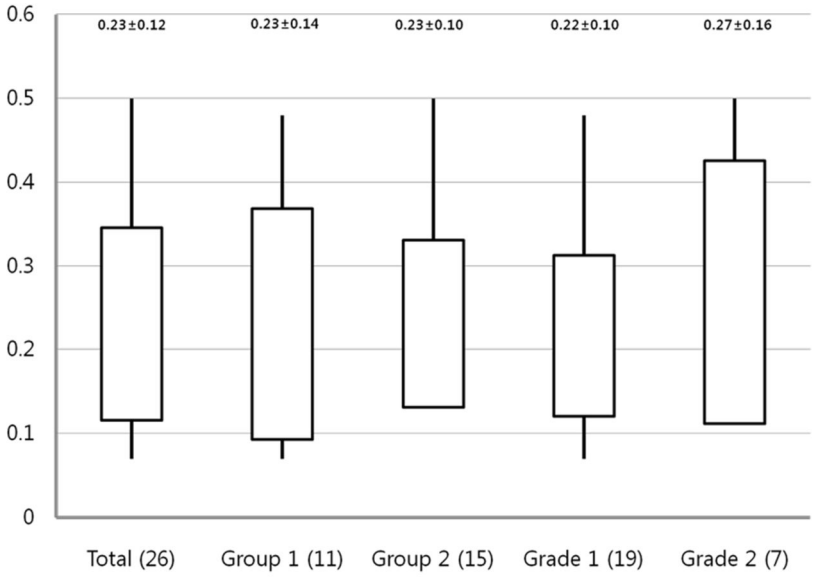

Figure 10. Fractional anisotropy (FA) within the solid-enhancing area of the meningioma

(y axis : FA of meningioma, Total : all 26 patients, Group 1 : 11 patients with weakness, Group 2 : 15 patients without weakness, Grade Ⅰ : WHO grade 1 meningioma, Grade Ⅱ : WHO grade 2 or 3 meningioma according to the WHO 2007 classification)

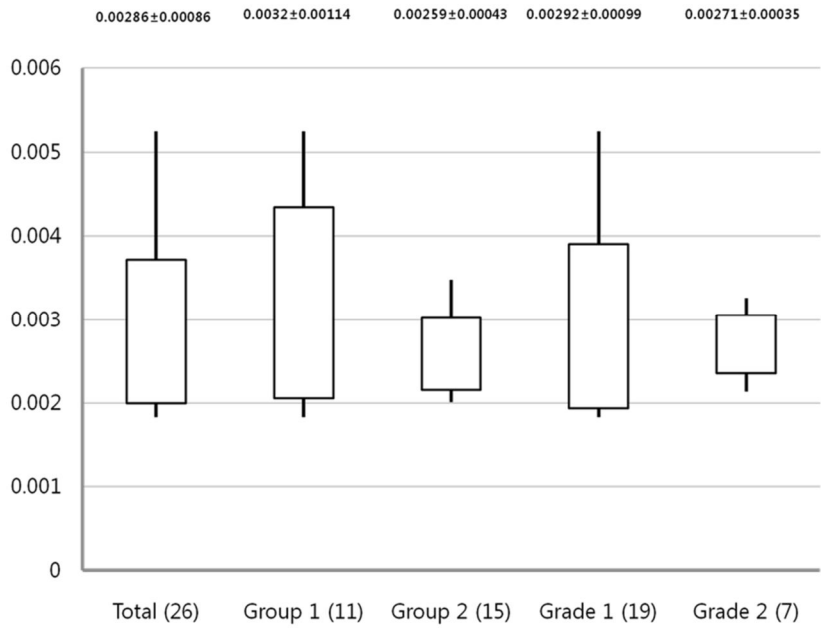

Figure 11. Tensor trace (TT) within the solid-enhancing area of the meningioma

(y axis : TT of the meningioma, (mm^2/s), Total : all 26 patients, Group 1 : 11 patients with weakness, Group 2 : 15 patients without weakness, Grade Ⅰ : WHO grade 1 meningioma, Grade Ⅱ : WHO grade 2 or 3 meningioma according to the WHO 2007 classification)

The ratios of FA and TT in the enhancing area of the meningioma and contralateral white matter are illustrated in Figures 12 and 13, respectively.

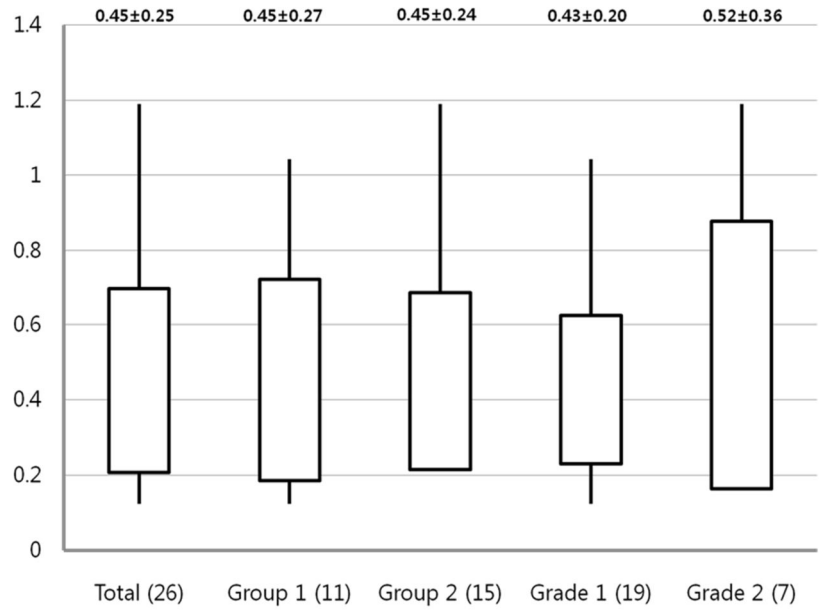

Figure 12. Fractional anisotropy (FA) ratios between the enhancing area of the meningioma and the contralateral white matter

(y axis : FA ratio of the meningioma, Total : all 26 patients, Group 1 : 11 patients with weakness, Group 2 : 15 patients without weakness, Grade Ⅰ : WHO grade 1 meningioma, Grade Ⅱ : WHO grade 2 or 3 meningioma according to the WHO 2007 classification)

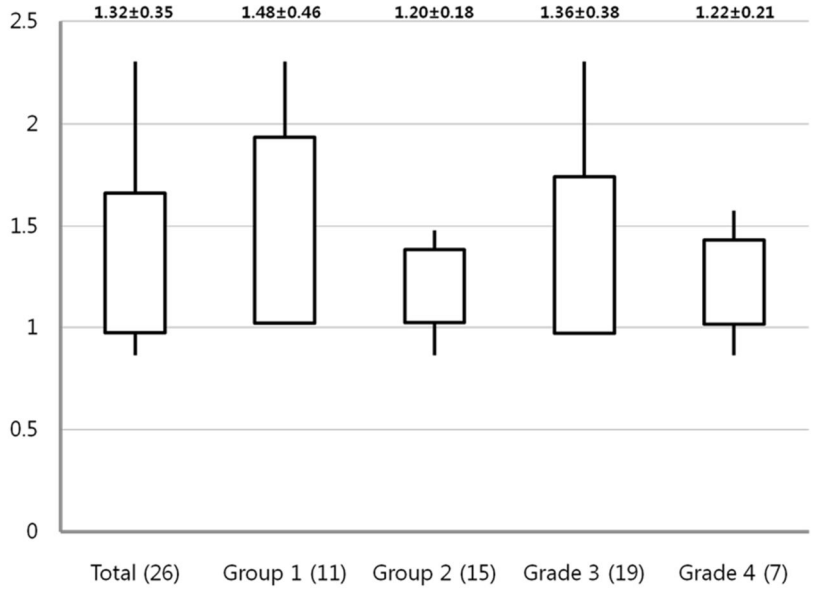

Figure 13. Tensor trace (TT) ratios between the enhancing area of the meningioma and the contralateral white matter

(y axis : TT ratio of the meningioma, Total : all 26 patients, Group 1 : 11 patients with weakness, Group 2 : 15 patients without weakness, Grade Ⅰ : WHO grade 1 meningioma, Grade Ⅱ : WHO grade 2 or 3 meningioma according to the WHO 2007 classification)

6. Conventional MRI

In Group 1, ten of the 11 patients showed edema or compression of the MC on T2 images. One patient without

edema or compression of the MC showed compression of the cerebral peduncle by the meningioma.

In Group 2, thirteen of the 15 patients showed no edema or compression of the MC. The remaining two patients showed edema and compression of the MC.

DISCUSSION

1. Diffusion parameters of the CST

Several studies have shown that the fiber tracts in the vicinities of brain tumors can be displaced, disrupted, or invaded by the tumor (6, 13–15). However, it is unclear how the directionality of water diffusion is affected in the peritumoral regions.

In the mouse, white matter tract $\lambda 1$ is typically 2–3fold larger than $\lambda 2$ and $\lambda 3$, reflecting the greater freedom of water to diffuse along the principal fiber axis rather than perpendicular to it (3), which is similar to that in the human brain. It has been shown in animal studies that the eigenvalues of the diffusion tensor ($\lambda 1$, $\lambda 2$ and $\lambda 3$) may vary differently between axonal injury and the dysmyelination/demyelination of the brain (3). It is possible that the directional diffusivities (i.e., eigenvlaues) may offer further insight into how myelin/axons are affected by disease. For example, it is reasonable to hypothesize that RD is more sensitive than AD to changes in myelin integrity. And Song et al. (3) reported that DTI results describe the effects of dysmyelination on the water directional diffusivities in the brains of shiverer mice.

Axonal fiber packing or compression by the tumor will affect both AD and RD. However, it is difficult to predict how this packing affect the directional diffusivities (3). A study by Schonberg et al. (13) showed that along fiber systems that are displaced and compressed as a result of brain tumors, the diffusivity increases parallel to the fibers and decreases perpendicular to them. This leads to an overall increase in FA and to the conclusion that this may reflect the compression of the fiber bundle (13). The results of Schonberg et al. are contrary to our data. However, in that study did not consider weakness when evaluating FA and TT measurements in the peritumoral white matter (13).

We hypothesize that TT value of peritumoral white matter is determined by a balance between factors decreasing the degree of water diffusion and those increasing it. And we have demonstrated that preoperative weakness in meningioma patients can be demonstrated by DTI data as reduced FA and elevated TT values. On the basis of our eigenvalue data, it can also be argued that the elevated TT values we observed in meningioma patients with weakness are attributable to increased diffusion perpendicular to the CST (as indicated by

the increased $\lambda 2$ and $\lambda 3$ values).

The dependence of FA on age has been described in a study by Salat et al. (16), who reported a reduction in FA of 0.2% per year within the PLIC. Yasmin et al. (17) evaluated FA of the bilateral CSTs of 100 healthy subjects and demonstrated no asymmetry. Yasmin et al. (17) also reported that the left–right ratio of MD in the bilateral CST ranged from 0.9726 to 0.9736 ($p<0.0001$). Therefore, we can ignore left–right asymmetry in the diffusion parameters of the CST in healthy subjects.

2. Diffusion parameter of the SLF

In our analysis of the diffusion parameters of the SLF, we did not consider the functional deficits associated with the SLF. The diffusion parameters of the SLF showed similar pattern to those of the CST in Group 1. AD of the SLF did not differ between the two hemispheres. TT and RD of the SLF on the lesioned side was higher (10%–14% increase, Figure 7) than those on the contralateral side and showed nearly half value the value of those (15%–33% increase, Figure 5) of the CST in Group 1. These values for the SLF explained by the fact that we did not consider the functional impairment associated with the SLF contrary to our analysis of the CST. If we can divide

meningioma patients into two groups according to SLF functional deficit, we will obtain very similar data with diffusion parameters of CST.

Kitamura et al.(18) reported that the mean FA and ADC value for the SLF did not differ significantly between the two hemispheres of 40 healthy elderly subjects. Therefore, in our study, the differences in the diffusion parameters of the SLF between the two hemispheres might demonstrate a true tumor-associated change.

3. Diffusion parameters of vasogenic edema

Peritumoral brain edema is found in approximately 50% of meningiomas (19). Vasogenic edema, classically associated with brain tumors, is produced by the entry of water into the brain tissue across leaky blood-brain and blood-tumor barriers. In a brain tumor model of vasogenic (leaky capillary) edema, the diffusion of an inert macromolecular fluorescent marker was reduced more than fourfold in hypercellular tumors and the surrounding astrogliotic tissue. However, the diffusion in the brain away from the tumor was ~30% faster than in the normal contralateral brain (20). Server et al. (21) reported that the ADC of peritumoral edema in meningiomas and high-grade

gliomas increased from 1.4 to 1.7. Some authors have analyzed the diffusion and FA of peritumoral edema in high-grade gliomas, meningiomas, lymphomas and metastases (21, 22), and these authors reported that the ADC values for peritumoral edema were higher than those for the contralateral normal white matter (23).

The mechanism by which meningiomas produce brain edema is as yet unclear. Tumor size, the location of the tumor, its histological type, the vascular supply to the tumor, and the level of prostaglandins, or sex hormones in the tumor have been reported to correlate with brain edema, but none of these has been proven to be a definite cause (24).

In evaluating conventional MR imaging, we identified MC edema in most meningioma patients with weakness. On next step, we evaluated the changes in the diffusion parameters for vasogenic edema, focusing on directional diffusivity. The diffusion in vasogenic edema increased in all three directions ($\lambda 1$, $\lambda 2$, and $\lambda 3$), and $\lambda 1$, $\lambda 2$, and $\lambda 3$ in vasogenic edema associated with meningioma were 58%-171% higher than those in the contralateral normal- appearing white matter (Figure 8).

In our study, we analyzed the CST and SLF separately. The

directional diffusivity of the CST in Group 1 and the SLF in meningioma patients showed data similar pattern to those produced by demyelination. White matter in vasogenic edema is composed by projection (e.g CST), association (e.g SLF), and commissural fiber (e.g corps callosum). Directional diffusivity in vasogenic edema may be sum of diffusion parameters of three different kinds of fiber with different direction. Also although the cause of peritumoral edema associated with meningioma is probably multifactorial (25), demyelination may contribute to some degree to the diffusion changes in the vasogenic edema associated with meningioma. But most important factor for diffusion parameters in vasogenic edema maybe water accumulation.

4. Clinical implications of peritumoral edema

Stereotactic radiosurgery has emerged as an effective surgical tool for managing intracranial meningiomas. Overall, radiosurgery-related complications have been reported in approximately 9% of patients (26, 27). The range of complications includes radiation necrosis, cranial nerve deficit, motor deficit, hydrocephalus, vascular occlusion, and the development of peritumoral edema (28). Zhao et al. (29)

demonstrated histopathological changes in the trigeminal nerve after Gamma Knife radiosurgery in rhesus monkeys. Nerve demyelination, degeneration, fragmentation, and loss of axons were observed. The delayed occurrence of adjacent edema is a well-known risk of using radiosurgery to manage intracranial meningiomas. It has been proposed that this complication may be related to several risk factors, including tumor location, tumor volume, and the total radiation dose (28).

In our study, we demonstrated that the white matter tract (CST and SLF) in the area of vasogenic edema associated with a meningioma showed changes in its diffusion parameters similar to those observed with demyelination. We think that radiosurgery may further damage the white matter tract already affected with pretreatment demyelination.

Conti et al. (30) reported the protection of venous structures during radiosurgery for parasagittal meningioma. They found that reducing the irradiation of the veins that course along the surface of the meningioma, which may be at risk of radiation-induced occlusion, is feasible in parasagittal meningioma radiosurgery. In the future, we may prevent or decrease radiation damage to the peritumoral edema in meningioma

patients by using a lower dose radiation or protecting any peritumoral edema from exposure to radiation.

5. Limitations of this study

Although the use of DTI and tractography is considered to be promising, our methods have some limitations. First, image distortion and the relatively lower signal-to-noise ratio of DTI represent major problems. The second limitation is that image reconstruction by tractography is not a precise stepwise procedure with a reproducible outcome, but is dependent on the manipulation of the ROIs. Because of these limitations, we believe that the quantitative estimation of the CST and SLF with fiber tracking may not be accurate.

Tracking results may change in regions with lower FA, such as tumor infiltrated areas or areas of crossing fibers, where the CST intersects with callosal fibers at the level of the centrum semiovale (31). In our study, fiber tracking was also unable to resolve crossing fiber pathways. Fiber tracking near the cortex or centrum semiovale is impossible because of crossing fibers, especially on the lateral side. Previous studies have suggested that fiber tracking of the motor tracts is inadequate in the lateral portions of the corticobulbar/spinal tract (32). Holodny

et al. (33) reported that the corticobulbar tract is probably too small to trace because when fibers cross, the fiber tracking algorithm will preferentially track the larger tract or stop fiber tracking for averaging of eigenvector in the voxel.

In our study, we also reached the limits of today's DTI fiber tracking technique. To further refine the setup developed in this study, we could develop and apply tracking algorithms that are based on diffusion data that resolve multiple fiber directions within the voxel. Higher-order mathematical tensor models, as proposed in other studies (34, 35), could provide a possible basis for these algorithms.

The relationship between demyelination and increase in RD is somewhat more complex for a variety of reasons. For instance, it is not yet clear whether RD is specific to demyelination in the presence of significant axonal damage or inflammation (4).

In this study, we used several types of MR units and several kinds of acquisition parameters of MR imaging for DTI. We used two methods to verify that the different MR units and parameters did not significantly influence the diffusion parameters. First, we analyzed the ratio of the diffusion parameters to evaluate the difference across the two

hemispheres of the same patient. Second, we analyzed whether the FA and TT of the meningiomas in our study had values similar to those reported in other studies.

Toh et al. (12) demonstrated that the mean (±SD) FA was 0.230±0.085 in solid-enhancing areas of classic meningiomas and 0.336±0.105 in atypical meningiomas. The mean (±SD) FA ratios (FA of meningioma/FA of contralateral white matter) of classic meningioma and atypical meningioma showed 0.45±0.16 and 0.66±0.19, respectively. They also showed that the mean (±SD) ADC was 0.000964±0.000172 (mean of TT is threefold of ADC, 0.000964X3 = 0.002892) in solid-enhancing areas of classic meningiomas and 0.000791±0.000129 (0.000791X3 = 0.002373) in atypical meningiomas. The mean (±SD) TT ratios (TT of meningioma/FA of contralateral white matter) of classic meningioma and atypical meningioma showed 1.27±0.24 and 1.05±0.17, respectively. In our results, FA and TT and ratios of FA and TT for the meningiomas (Figures 10-13) were compatible with the results of Toh et al. (12), despite the several types of MR units and several kinds of acquisition parameters for MR imaging used.

In this study of patient with meningioma, the lesion-side CST of the patients with weakness showed reductions in FA, an increase in TT resulting from increased RD, and no change in AD. These results are similar to those observed with demyelination. And directional diffusivity of the SLF showed similar pattern but less degree than those of the lesion-side CST. The diffusion data for the peritumoral edema adjacent to the meningioma showed increased diffusion in both AD and RD and showed larger changes than those in the CST of Group 1 or in the SLF of all the patients with meningioma. These results suggest that the diffusion parameters in vasogenic edema are partly influenced by demyelination.

REFERENCES

1. Berman JI, Mukherjee P, Partridge SC, Miller SP, Ferriero DM, Barkovich AJ, et al. Quantitative diffusion tensor MRI fiber tractography of sensorimotor white matter development in premature infants. Neuroimage. 2005 Oct; 27(4): 862-71.

2. Nagesh V, Tsien CI, Chenevert TL, Ross BD, Lawrence TS, Junick L, et al. Radiation-induced changes in normal-appearing white matter in patients with cerebral tumors: a diffusion tensor imaging study. Int J Radiat Oncol Biol Phys. 2008 Mar; 70(4): 1002-10.

3. Song SK, Sun SW, Ramsbottom MJ, Chang C, Russell J, Cross AH. Dysmyelination revealed through MRI as increased radial (but unchanged axial) diffusion of water. Neuroimage. 2002 Nov; 17(3): 1429-36.

4. Budde MD, Xie M, Cross AH, Song SK. Axial diffusivity is the primary correlate of axonal injury in the experimental autoimmune encephalomyelitis spinal cord: a quantitative pixelwise analysis. J Neurosci. 2009 Mar; 29(9): 2805-13.

5. Virta A, Barnett A, Pierpaoli C. Visualizing and

characterizing white matter fiber structure and architecture in the human pyramidal tract using diffusion tensor MRI. Magn Reson Imaging. 1999 Oct; 17(8): 1121-33.

6. Field AS, Alexander AL, Wu YC, Hasan KM, Witwer B, Badie B. Diffusion tensor eigenvector directional color imaging patterns in the evaluation of cerebral white matter tracts altered by tumor. J Magn Reson Imaging. 2004 Oct; 20(4): 555-62.

7. Andersen C, Jensen FT. Differences in blood-tumour-barrier leakage of human intracranial tumours: quantitative monitoring of vasogenic oedema and its response to glucocorticoid treatment. Acta Neurochir (Wien). 1998; 140(9): 919-24.

8. Bastin ME, Sinha S, Whittle IR, Wardlaw JM. Measurements of water diffusion and T1 values in peritumoural oedematous brain. Neuroreport. 2002 Jul; 13(10): 1335-40.

9. Fillmore HL, VanMeter TE, Broaddus WC. Membrane-type matrix metalloproteinases (MT-MMPs): expression and function during glioma invasion. J Neurooncol. 2001 June; 53(2): 187-202.

10. Ikuta F, Yoshida Y, Ohama E, Oyanagi K, Takeda S,

Yamazaki K, et al. Revised pathophysiology on BBB damage: the edema as an ingeniously provided condition for cell motility and lesion repair. Acta Neuropathol Suppl. 1983; 8: 103-10.

11. Mori S, Frederiksen K, van Zijl PC, Stieltjes B, Kraut MA, Solaiyappan M, et al. Brain white matter anatomy of tumor patients evaluated with diffusion tensor imaging. Ann Neurol. 2002 Mar; 51(3): 377-80.

12. Toh CH, Castillo M, Wong AM, Wei KC, Wong HF, Ng SH, et al. Differentiation between classic and atypical meningiomas with use of diffusion tensor imaging. AJNR Am J Neuroradiol. 2008 Oct; 29(9): 1630-5.

13. Schonberg T, Pianka P, Hendler T, Pasternak O, Assaf Y. Characterization of displaced white matter by brain tumors using combined DTI and fMRI. Neuroimage. 2006 May; 30(4): 1100-11.

14. Smits M, Vernooij MW, Wielopolski PA, Vincent AJ, Houston GC, van der Lugt A. Incorporating functional MR imaging into diffusion tensor tractography in the preoperative assessment of the corticospinal tract in patients with brain tumors. AJNR Am J Neuroradiol. 2007 Aug; 28(7): 1354-61.

15. Bello L, Gambini A, Castellano A, Carrabba G, Acerbi F,

Fava E, et al. Motor and language DTI Fiber Tracking combined with intraoperative subcortical mapping for surgical removal of gliomas. Neuroimage. 2008 Jan; 39(1): 369-82.

16. Salat DH, Tuch DS, Greve DN, van der Kouwe AJ, Hevelone ND, Zaleta AK, et al. Age-related alterations in white matter microstructure measured by diffusion tensor imaging. Neurobiol Aging. 2005 Aug-Sep; 26(8): 1215-27.

17. Yasmin H, Aoki S, Abe O, Nakata Y, Hayashi N, Masutani Y, et al. Tract-specific analysis of white matter pathways in healthy subjects: a pilot study using diffusion tensor MRI. Neuroradiology. 2009 Dec; 51(12): 831-40.

18. Kitamura S, Morikawa M, Kiuchi K, Taoka T, Fukusumi M, Kichikawa K, et al. Asymmetry, sex differences and age-related changes in the white matter in the healthy elderly: a tract-based study. BMC Res Notes. 2011 Oct; 4: 378.

19. Kalkanis SN, Carroll RS, Zhang J, Zamani AA, Black PM. Correlation of vascular endothelial growth factor messenger RNA expression with peritumoral vasogenic cerebral edema in meningiomas. J Neurosurg. 1996 Dec; 85(6): 1095-101.

20. Papadopoulos MC, Binder DK, Verkman AS. Enhanced macromolecular diffusion in brain extracellular space in mouse

models of vasogenic edema measured by cortical surface photobleaching. FASEB J. 2005 Mar; 19(3): 425-7.

21. Server A, Kulle B, Maehlen J, Josefsen R, Schellhorn T, Kumar T, et al. Quantitative apparent diffusion coefficients in the characterization of brain tumors and associated peritumoral edema. Acta Radiol. 2009 Jul; 50(6): 682-9.

22. van Westen D, Latt J, Englund E, Brockstedt S, Larsson EM. Tumor extension in high-grade gliomas assessed with diffusion magnetic resonance imaging: values and lesion-to-brain ratios of apparent diffusion coefficient and fractional anisotropy. Acta Radiol. 2006 Apr; 47(3): 311-9.

23. Toh CH, Wong AM, Wei KC, Ng SH, Wong HF, Wan YL. Peritumoral edema of meningiomas and metastatic brain tumors: differences in diffusion characteristics evaluated with diffusion-tensor MR imaging. Neuroradiology. 2007 Jun; 49(6): 489-94.

24. Nakano T, Asano K, Miura H, Itoh S, Suzuki S. Meningiomas with brain edema: radiological characteristics on MRI and review of the literature. Clin Imaging. 2002 Jul-Aug; 26(4): 243-9.

25. Lee KJ, Joo WI, Rha HK, Park HK, Chough JK, Hong YK,

et al. Peritumoral brain edema in meningiomas: correlations between magnetic resonance imaging, angiography, and pathology. Surg Neurol. 2008 Apr; 69(4): 350-5; discussion 5.

26. Flickinger JC, Kondziolka D, Maitz AH, Lunsford LD. Gamma knife radiosurgery of imaging-diagnosed intracranial meningioma. Int J Radiat Oncol Biol Phys. 2003 Jul; 56(3): 801-6.

27. Pollock BE. Stereotactic radiosurgery for intracranial meningiomas: indications and results. Neurosurg Focus. 2003 May; 14(5): e4.

28. Patil CG, Hoang S, Borchers DJ, 3rd, Sakamoto G, Soltys SG, Gibbs IC, et al. Predictors of peritumoral edema after stereotactic radiosurgery of supratentorial meningiomas. Neurosurgery. 2008 Sep; 63(3): 435-40; discussion 40-2.

29. Zhao ZF, Yang LZ, Jiang CL, Zheng YR, Zhang JW. Gamma Knife irradiation-induced histopathological changes in the trigeminal nerves of rhesus monkeys. J Neurosurg. 2010 Jul; 113(1): 39-44.

30. Conti A, Pontoriero A, Salamone I, Siragusa C, Midili F, La Torre D, et al. Protecting venous structures during radiosurgery for parasagittal meningiomas. Neurosurg Focus.

2009 Nov; 27(5): E11.

31. Okada T, Mikuni N, Miki Y, Kikuta K, Urayama S, Hanakawa T, et al. Corticospinal tract localization: integration of diffusion-tensor tractography at 3-T MR imaging with intraoperative white matter stimulation mapping--preliminary results. Radiology. 2006 Sep; 240(3): 849-57.

32. Clark CA, Barrick TR, Murphy MM, Bell BA. White matter fiber tracking in patients with space-occupying lesions of the brain: a new technique for neurosurgical planning? Neuroimage. 2003 Nov; 20(3): 1601-8.

33. Holodny AI, Watts R, Korneinko VN, Pronin IN, Zhukovskiy ME, Gor DM, et al. Diffusion tensor tractography of the motor white matter tracts in man: Current controversies and future directions. Ann N Y Acad Sci. 2005 Dec; 1064: 88-97.

34. Frank LR. Anisotropy in high angular resolution diffusion-weighted MRI. Magn Reson Med. 2001 Jun; 45(6): 935-9.

35. Frank LR. Characterization of anisotropy in high angular resolution diffusion-weighted MRI. Magn Reson Med. 2002 Jun; 47(6): 1083-99.

초록

서론: 확산텐서영상은 뇌안에서 물분자의 확산특성을 보여주기 위해서 최근에 도입되었다. 확산텐서영상으로 측정되는, 신경섬유와 평행한 방향의 확산정도 (축성확산정도, AD, $\lambda 1$)의 감소는 축삭의 손상을 나타낸다. 또한 신경섬유와 직각 방향의 확산정도 (방사상확산정도, RD [$\lambda 2$ 와 $\lambda 3$])의 증가는 탈수초의 특징적인 소견이다. 저자들은 수막종을 가지고 있는 환자에서 피질척수로, 위세로다발, 혈관기인성부종에서의 확산정도를 측정하였다. 각각의 섬유로 및 혈관기인성부종에서 관찰되는 축삭의 손상과 탈수초를 감별하고, 종양주위부종의 발생기전을 유추하였다.

방법: 수막종을 가진 26 명의 환자가 이 연구에 포함되었다. 다발성 수막종이나 양쪽 대뇌반구에 수막종이 위치한 경우는 제외하였다. 근위약을 보인 11 명의 환자는 1 군으로, 근위약이 없는 15 명의 환자는 2 군으로 분류하였다. DTIStudio 프로그램을 이용하여 피질척수로와 위세로다발에 대한 신경섬유로추적을 시행하였다. 또한 혈관기인성부종과 관심지역 (ROI)의 위치에 따라서는, 관심지역이 혈관기인성부종에 위치한 3 군과 정상 종양주위백색질에 위치한 4 군으로 나누었다. 신경섬유로추적을 통해 만들어진 피질척수로와 위세로다발의 확산계수는 DTIStudio 의 tract

statistics 기능을 이용하여 분석하였다. 분석에 포함된 확산계수는 분획비등방성 (FA), 긴장 흔적 (TT), AD 와 RD 였다. 확산계수는 수막종이 위치한 대뇌반구의 값과 반대쪽 대뇌반구의 값의 비를 one-sample T-test 를 이용하여 분석하였다.

결과: 피질척수로의 확산계수는, 1 군에서는 수막종이 위치한 대뇌반구에서 FA (15% 감소), TT 와 RD (15%-33% 증가)는 반대쪽 대뇌반구의 값과 차이를 보였으나, AD 는 차이가 없었다. 한편 2 군에서는 피질척수로의 FA 와 $\lambda 3$ 는 양쪽 대뇌반구에서 차이가 없었고, TT, $\lambda 1$ 과 $\lambda 2$ 는 반대쪽 대뇌반구의 값보다 증가 (3%-10%)하였다. 그러나, 그 차이의 정도는 작았다. 위세로다발의 섬유로추적은 22 명에서만 가능하였다. 수막종이 위치한 대뇌반구 위세로다발의 FA (6% 감소), TT 와 RD (10%-14% 증가)는 반대쪽 대뇌반구와 차이를 보였다. 또한 이 값은 1 군의 피질척수로에서 보이는 양쪽 대뇌반구의 차이보다 작았다. 위세로다발의 AD 는 양쪽 대뇌반구에서 차이가 없었다. 관심지역이 혈관기인성부종에 위치한 3 군에서는 부종의 확산계수가 반대쪽 정상으로 보이는 백색질의 확산계수와는 세 방향 모두에서 많은 차이를 보였고 (FA 는 38%감소, TT, AD 와 RD 는 58-171%증가), 이 차이는 1 군의 피질척수로에서의 확산계수 차이보다 더 큰 값이었다. 수막종과 같은 쪽 대뇌반구의 정상으로

보이는 백색질의 확산계수는 반대쪽 백색질의 확산계수와 차이가 없었다.

결론: 수막종 환자에서 근력의 위약은 피질척수로의 FA, TT, RD 의 차이와 연관되어 있고 AD 와는 관련이 없다. 위세로다발의 확산정도와 1 군의 피질척수로는 탈수초에서 보이는 확산계수의 변화와 유사한 패턴을 보인다. 또한 혈관기인성부종의 확산계수의 변화는 부종의 형성에 탈수초가 관여하는 것을 시사한다.

주요어 : 확산텐서영상, 혈관기인성부종, 확산계수, 피질척수로, 위세로다발

학 번 : 2002-31135

서울대학교 대학원

의학과 신경외과학 과정

김명수